

Study of Anodic Oxide Films of Titanium Fabricated by Voltammetric Technique in Phosphate Buffer Media

Madhav Prasad Neupane¹, Il Song Park², Sook Jeong Lee³, Kyoung A Kim⁴, Min Ho Lee^{2,*}, Tae Sung Bae²

¹ Department of Bionanosystem Engineering, Chonbuk National University, Jeonju 561-756, Republic of Korea

² Department of Dental Biomaterials and Institute of Oral Bioscience, School of Dentistry, Chonbuk National University, Jeonju 561-756, Republic of Korea

³ Neural Injury Research Lab, Department of Neurology, Asan Life Science Institute, University of Ulsan, College of Medicine, Seoul 138-736, Republic of Korea

⁴ Department of Oral and Maxillofacial Radiology and Institute of Oral Bioscience, School of Dentistry, Chonbuk National University, Jeonju 561-756, Republic of Korea

*E-mail: LMH@chonbuk.ac.kr

Received: 18 September 2008 / Accepted: 10 January 2009 / Published: 9 February 2009

The corrosion process is one of the main factors affecting the biocompatibility and mechanical integrity of an implant material. This study examined the anodic oxide films produced on titanium metal using cyclic voltammetric method. The oxide films were produced potentiodynamically at room temperature from a potential ranging from -1.0 to +5.0 V, at a scan rate of 50mVs⁻¹ in a phosphate buffer solution at pH 2, 7, and 12. After oxide growth, the films were subjected to different repetitive potentiodynamic cycles at 50mVs⁻¹ between the pre-set cathodic and anodic potentials. The changes in the electrochemical behaviour of the passive electrode, particularly the corrosion of the metal were followed as a function of the electrolyte pH and the number of potentiodynamic cycles. The corrosion of metal surface was severe at pH 2 and increases with increasing number of cycles whereas invariable at pH 7 and in decreasing order at pH 12 as the number of cycle increased. In addition, the surface roughness of modified surfaces was varied as like corrosion of metal as the number of cycles increased.

Keywords: Biocompatibility, anodic oxide, corrosion, osseointegration

1. INTRODUCTION

Titanium and its alloys are the most popular implant materials in the biomedical field on account of their excellent biocompatibility characteristics such as chemical stability, mechanical

resistance and absence of toxicity. The aerospace and chemical industries are also taking advantage of these characteristics. Corrosion is a critical process in metallic implants because it can adversely affect the biocompatibility and mechanical integrity of a biomaterial. Corrosion and dissolution of the surface film of an implant are two of the most important mechanisms for introducing foreign ions into the body, which can have adverse biological effects [1, 2]. There have been considerable efforts to improve the osseointegration capability of titanium implants by enhancing the level of osteoconduction on their surfaces by modifying the surface morphology and chemistry.

Many surface modification treatments have been studied in an attempt to improve the corrosion behavior of metallic biomaterials, as well as their biocompatibility and mechanical properties [3–5]. Among them, powder/fiber/wire mesh metallurgical sintering [6, 7], plasma spray processing [8, 9], electrochemical oxidation, sol-gel deposition [10], and surface blasting [11] are some methods commonly used to modify the surface topography of load-bearing titanium. Titanium has the characteristics of other valve metals because of its coherent and not easily reducible oxide layer on its surface. In valve metals, the growth of anodic films are commonly irreversible, and occur with a fixed stoichiometry under an electrical field strength and current density described by the high field model: $j=A \exp(\beta\varepsilon)$, where j is the anodic current density, ε is the electric field and A and β are the material dependent constants [12,13]. On the other hand, the nature of the forming electrolyte solution and its pH also affect the stability, composition and thickness of the anodically grown oxide films [14-17]. The electrochemical oxidation of titanium has been examined in different electrolytic media using different techniques such as anodization and cyclic voltametry. During anodic oxidation, different types of titanium oxides (TiO , TiO_2 , Ti_2O_3 and Ti_3O_5) may be formed on the titanium surface in which TiO_2 is the most stable and frequently found oxide film [14,18] but the properties of the oxide depend on the method of preparation. Titanium oxide films are usually prepared using an anodic oxidation technique because it is cost effective and oxide formed by this method has good adhesion strength with titanium substrate. However, a voltammetric technique can also be used to form oxide films on valve metals. There are few reports on the production of oxide films using this technique. De Pauli et al. examined the effect of the number of potential cycles on the thin titanium oxide films formed on titanium in Na_2SO_4 solutions at pH 4.0 [19]. Bonilha and Zinolla [20] reported the electrochemical behavior of titanium electrodes in 0.1 mol l^{-1} KOH in the dark or under UV light. Fast repetitive potentiodynamic cycles were used to examine the potentiodynamic growth and reduction of films. Many studies have reported the changes in the physical properties of valve-metal oxides due to different perturbations occurring during their formation. Blackwood et al [16] investigated the stability of anodic films formed potentiodynamically on titanium in 3 mol l^{-1} H_2SO_4 . Blackwood and Peter [21] also reported the growth stability of anodic oxide films on titanium. Müller et al. [22] examined the stability of the oxide on titanium electrodes in 1 mol l^{-1} NaOH and in 0.5 mol l^{-1} H_2SO_4 using potentiodynamic experiments.

This study investigated the anodic films grown potentiodynamically on titanium in a 0.1M phosphate buffer solution at pH 2, 7 and 12, at low voltages and at room temperature. The different repetitive potentiodynamic triangular cycles were applied to the pre-formed anodic oxide.

2. EXPERIMENTAL PART

Commercially pure titanium plates grade 2 (20×10×2mm) were polished with SiC paper from 220 to 600 grit, ultrasonically cleaned, and dried. Cyclic voltammetry (CV) was performed using a conventional three-electrode cell with a titanium plate as the working electrode, a platinum electrode as the counter electrode and a Ag/AgCl (sat'd. KCl) as the reference electrode. The aqueous phosphate buffer electrolyte solutions were prepared using phosphoric acid and its potassium salts (KH₂PO₄ and K₂HPO₄), at pH of 2, 7 and 12 of concentration 0.1M, respectively.

A commercial potentiostat (EQCM, Shin EQCN1000, and Korea) was used for all electrochemical investigations and the data were recorded using an ECB (model RB 400) X-Y plotter. The anodic oxides were obtained potentiodynamically at scan rate of 50mVs⁻¹ in the potential range from -1.0 V to +5.0 V. After oxide growth, different repetitive CV cycles (5, 10 and 15) at sweep rate 50mVs⁻¹ were applied between pre-set cathodic and anodic potentials.

The surface morphology and microstructure were investigated by scanning electron microscopy (SEM, JEOL JSM-5900, Japan) equipped with an Energy Dispersive X-ray Spectrometer (EDS) (Oxford, England). The surface crystalline structure was examined by X-ray diffraction (XRD, Dmax III-A type, Rigaku Co., Japan) with Cu K α incident radiation. The surface roughness of the material was measured using a Surftest Formtracer (Surftest SV-402, Mitutoyo Instruments, Tokyo, Japan).

3. RESULTS AND DISCUSSION

3.1. Voltammetric study

Titanium electrodes exposed to the atmosphere after mechanical polishing are covered spontaneously by an oxide film. As soon as cyclic voltammetry was performed in phosphate buffer solution at different pH between potentials -1.0 and +5.0 V, the process of dissolution of natural oxide film of TiO₂ begins first. Simultaneously, self- passivated film formation also begins. This potential range was chosen because it encompasses all the electrochemical processes of interest in this work. Figure 1 show the cyclic voltammograms (CV) recorded at 50 mVs⁻¹ for titanium oxide growth in phosphate buffer solution at pH 2, 7, and 12, respectively. No changes in the anodic scan were observed. The similarity in the voltammograms at the three different pH is a clear indication that the surface preparation of the electrode and experimental conditions are quite reproducible. A uniform oxide layer begins to form (mainly TiO₂) during anodic oxidation [16, 21, 23, 24], which inhibits the dissolution of titanium according to the following reaction.



Ti₂O₃ may also be formed [25] but is unstable and rapidly transforms to TiO₂ when it comes in contact with water.



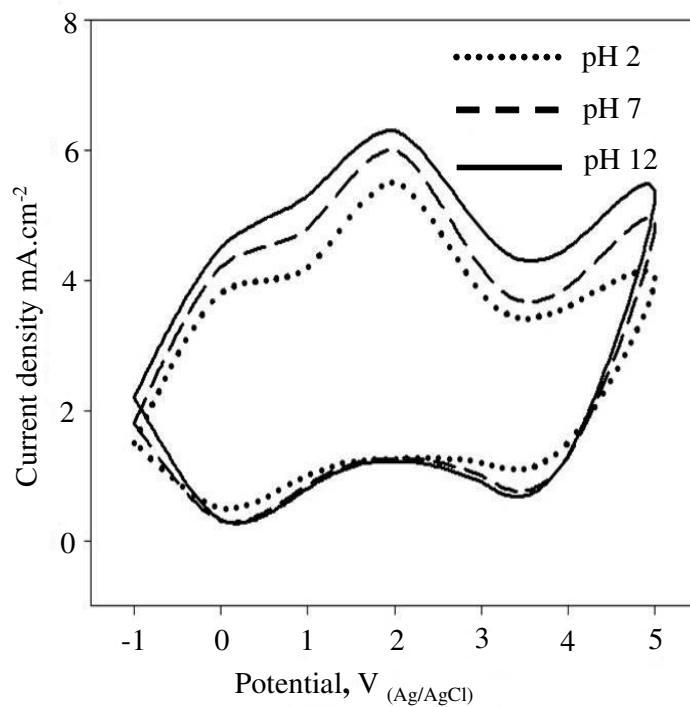


Figure 1. Comparative Cyclic voltammograms of the Ti electrode in a phosphate buffer solution at 0.1 Vs^{-1} scan rate at different pH

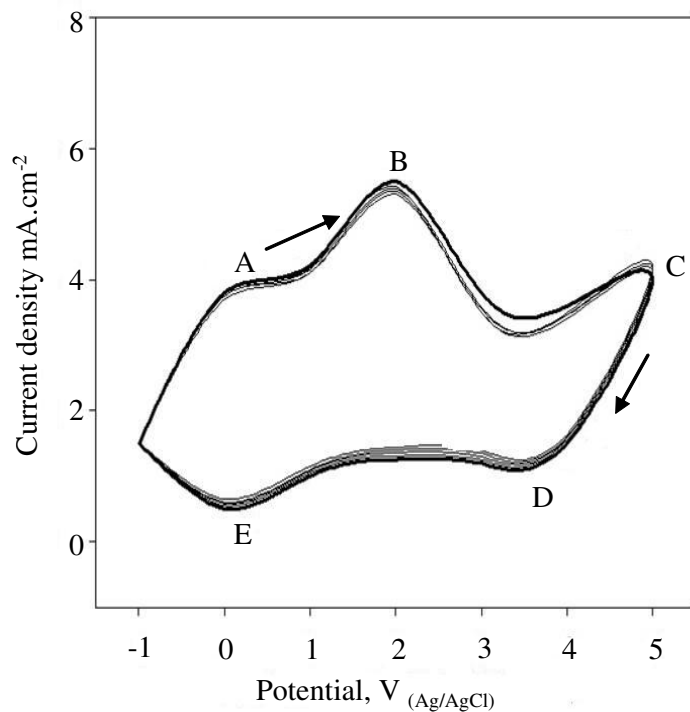


Figure 2. Successive cyclic voltammograms between -1.0 V to 5.0 V, at 50 mV s^{-1} , of a passive Ti electrode in a phosphate buffer solution at pH 2.0, as a function of the number of cycles

An anodic current peak can be observed at ≈ 2.0 V in each case. In the voltammogram obtained after approximately 2.0 V, a slight decrease of anodic current as the potential becomes more positive is noticed, most probably due to a decrease of the real surface area as the film thickness increases. In the lower part of the voltammograms the anodic current rapidly decreases at first, and then decreases slowly to approach zero. The small peaks in the lower part are due to the reduction of a secondary unstable species. Anodic transformations similar to that found for titanium at 2.3 V have also been reported for other valve metals [26, 27]. There has been considerable debate regarding the mechanism for the above phenomenon. Di Quarto et al. [26] attributed this current increase to the start of oxygen evolution when niobium is placed in a sulphuric acid solution, even though no significant oxygen evolution was observed. On the other hand, Schultze and co-workers [28, 29] found quite different oxide growth rates on different single grains of a titanium polycrystalline substrate at potentials > 3 V and also in sulphuric acid solutions. Recently, we reported that the increase in anodic current on passive titanium at 2.0 V might be due to an oxide phase transformation: in aged oxide films that are obtained potentiodynamically up to potentials that more positive than those in the 'hump' region. XRD indicated the presence of a TiO_2 matrix. Systematic studies using other surface techniques are currently underway in an attempt to better understand this phenomenon.

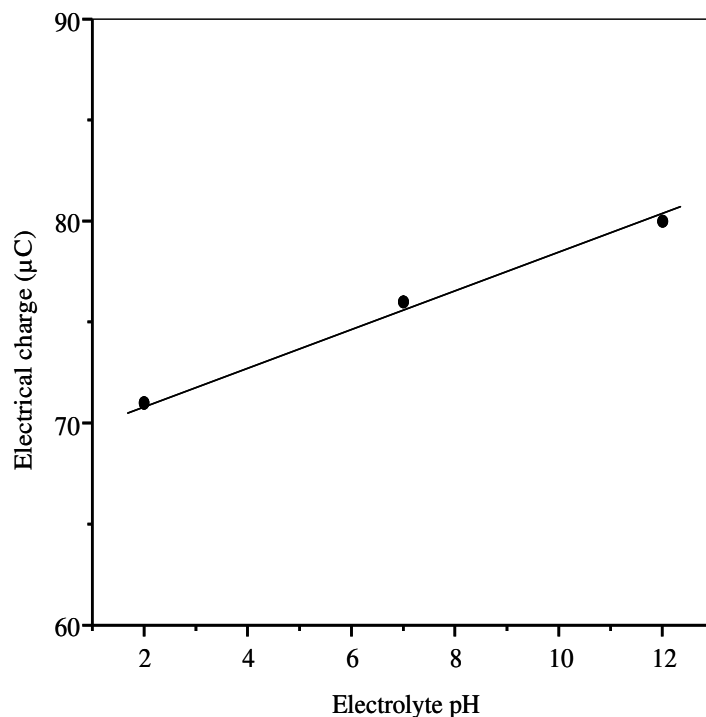


Figure 3. Electrical charge vs. electrolyte pH for cyclic voltammogram obtained in the 0.1M phosphate buffer solution

The effect of number of repetitive potentiodynamic cycles on previously grown oxide film was shown in figure 2. Five different repetitive cycles were carried out at pH 2 solution. After reaching the cathodic potential value of -1.0 V, the sweeps were reversed (made anodic again) and two important

features in the potentiodynamic profile of the anodic film were observed. The first is that an anodic peak at approximately 2.0 V is always present, and independent experiments showed that the total charge is dependent on the value of the cathodic potential. This peak has been attributed to the oxidation of hydrogen-containing species that accumulated in the oxide matrix during the cathodic sweep through the hydrogen evolution region [19]. Camara et al. [30] also reported a similar peak for titanium in Na_2SO_4 solutions at various pHs, and interpreted it to be due to the possible oxidation of non-stoichiometric species in the TiO_2 matrix, which had been formed during the cathodic sweep through the hydrogen evolution region. The other important feature drawn from Figure 2 is the continuous increase in anodic current from -1.0 V to +2.0 V with increasing number of potential cycles. The measured anodic current for anodized titanium, in the -1.0 to +5.0 V range, is the sum of two anodic contributions, i.e. one from the reconstruction of the dissolved or reduced oxide during the cathodic excursion and another from the oxygen evolution reaction. Similar profiles were obtained for the other repetitive cycles and pH values. Therefore, the film consists of a crystalline compact layer underlying a hydrous amorphous external layer. Both layers undergo different modifications with the external conditions applied to the passive electrode. The increase in electrical charge with increased electrolyte pH can be seen from the relation between electrical charge and electrolyte pH in figure 3. This relation is quite linear and shows only one slope. This behavior seems to indicate more electrical charge is needed if the electrolyte pH increases. These results clearly show that the oxide thickness increases with increasing potential because the charge is directly related to the oxide thickness. Furthermore, this increase is quite linear, which agrees with the growth behavior predicted by the high field growth model [31].

3.2. Scanning Electron Microscopy

The surface was examined by SEM at different stages of oxidation in order to understand the surface morphology of the anodic oxide film formed on pure titanium metal in phosphate buffer solution. SEM images of the pure titanium samples were taken before electrochemical oxidation to determine the differences in surface morphology after oxidation. After the oxide growth they were subjected to different repetitive CV cycles 5, 10 and 15 between the potentials of -1.0 and +5.0 V in a 0.1 M electrolyte solution at different pH, exhibited variations in surface morphology. SEM analysis revealed that the corrosion process was more severe on the titanium surface at pH 2 as the number of cycle increased (Figures 4a, 4b and 4c). Uniform corroded surface was seen at higher cycles (Figure 4c). This suggests that at low pH, the solution attacks the metal surface quite readily. Titanium in acidic medium, leads corrosion due to destruction of their passivity and loss of mechanical properties. However, at pH 7, there was no any differences in the corrosion of pure titanium regardless of the number of potentiodynamics cycles used (Figures 4d, 4e, and 4f). This is because there is very slow reaction with metals in a neutral solution. At pH 12, the level of corrosion damage decreased with increasing number of cycles (Figures 4g, 4h and 4i). This suggests that at alkaline pH passivation takes place. Passivity is caused by a change in anodic reaction. The formation of free metal ions gives way to a reaction which forms and insoluble film on the metal surface. These micrographs clearly show the

rough passive films with globular morphology. These micrographs also indicate that the intensity of corrosion damage was high at acidic pH and was a function of the number of potentiodynamic cycles. Similarly, the intensity of corrosion damage of titanium was similar at neutral pH and decreases at alkaline pH with increasing number of potentiodynamic cycles.

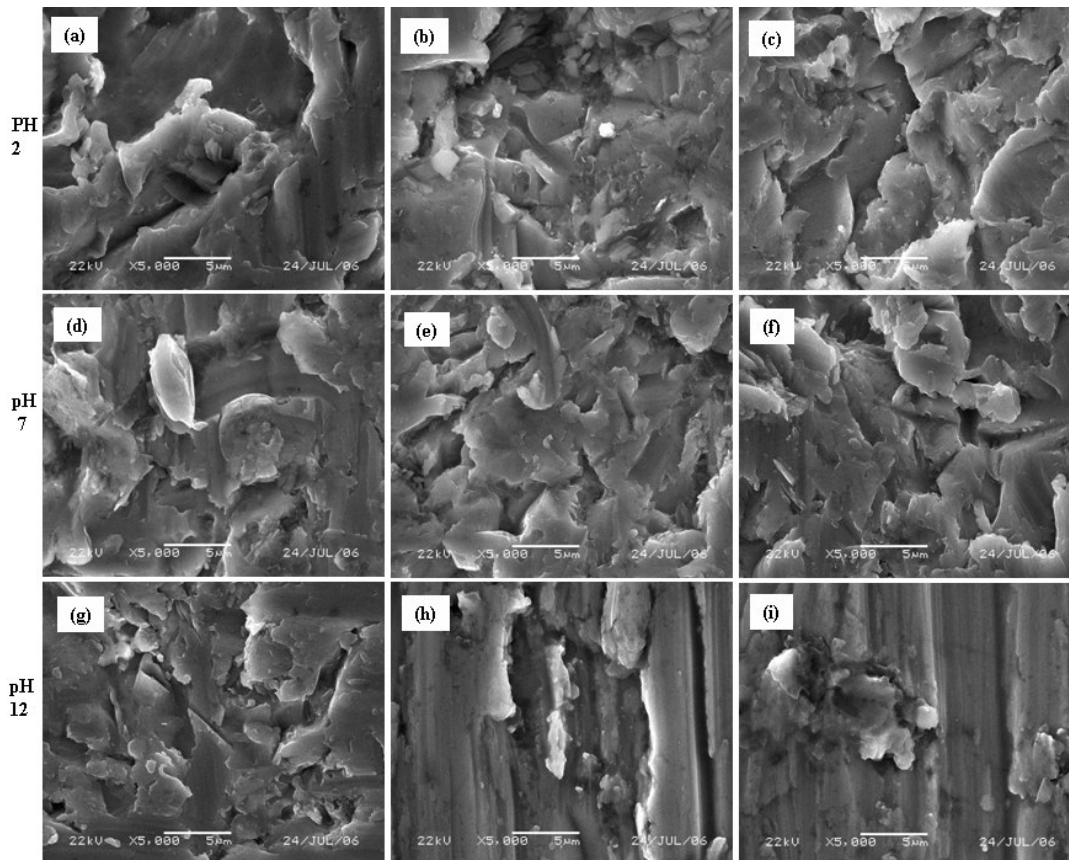


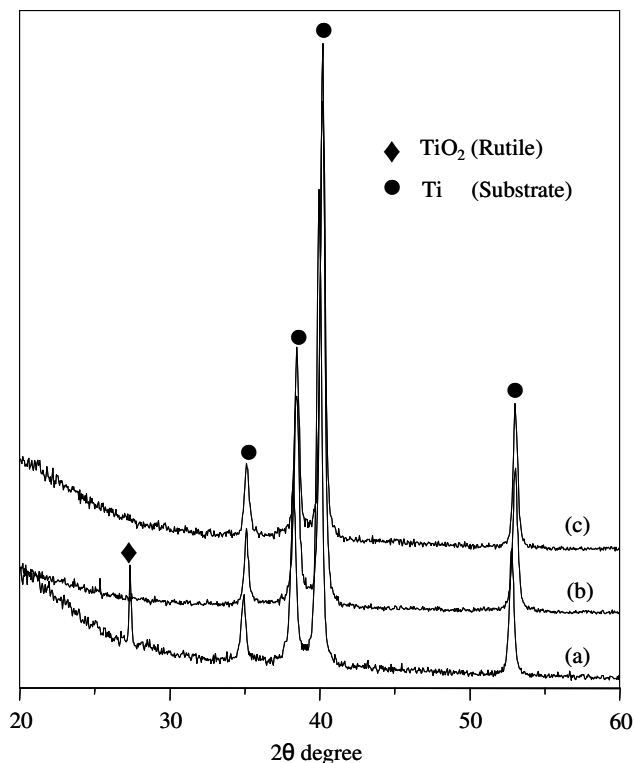
Figure 4. SEM micrographs of the Ti oxide formed in the phosphate buffer solution at different pH and different successive potential cycles, pH 2 (a) 5 (b) 10 (c) 15 cycles, pH 7 (d) 5 (e) 10 (f) 15 cycles, and pH 12 (g) 5 (h) 10 (i) 15 cycles

Table 1 shows surface roughness of different sample groups. Average surface roughness (R_a) was $0.250\mu\text{m}$, $0.328\mu\text{m}$ and $0.407\mu\text{m}$ for anodized sample at pH 2, $0.317\mu\text{m}$, $0.315\mu\text{m}$ and $0.309\mu\text{m}$ for anodized sample at pH 7 and $0.278\mu\text{m}$, $0.214\mu\text{m}$ and $0.170\mu\text{m}$ for anodized sample at pH 12 at different repetitive cycles 5, 10 and 15, respectively. With comparisons of the roughness of different groups, R_a value showed differences as the electrolyte pH and number of potentiodynamic cycles varied. This shows that the surface roughness of the oxide coating increases with increasing number of repetitive cycles in acidic pH, shows no change regardless of the number of cycles at neutral pH, and decreases at highly alkaline pH. This indicated that average surface roughness (R_a) of anodized sample is a function of electrolyte pH and number of potentiodynamic cycles.

Table 1. Roughness parameters obtained for Ti electrode in 0.1M phosphate buffer solution with different pH values at different sweep rate

Specimen	pH of electrolyte	Repetitive Cycles	Roughness \pm SD		
			Ra (μm)	Ry (μm)	Rz (μm)
1	2	5	0.250 \pm 0.006	1.751 \pm 0.031	1.202 \pm 0.007
2	2	10	0.328 \pm 0.006	2.194 \pm 0.006	1.762 \pm 0.006
3	2	15	0.407 \pm 0.019	3.400 \pm 0.008	1.872 \pm 0.041
4	7	5	0.317 \pm 0.004	2.088 \pm 0.062	1.467 \pm 0.005
5	7	10	0.315 \pm 0.011	3.023 \pm 0.017	1.753 \pm 0.005
6	7	15	0.309 \pm 0.001	2.124 \pm 0.013	1.692 \pm 0.002
7	12	5	0.278 \pm 0.004	2.248 \pm 0.024	1.703 \pm 0.008
8	12	10	0.214 \pm 0.010	1.999 \pm 0.057	1.448 \pm 0.017
9	12	15	0.170 \pm 0.006	1.981 \pm 0.040	1.013 \pm 0.094

n=3, SD=Standard Deviation

**Figure 5.** XRD peaks of the specimens treated electrochemically by cyclic voltametry for (a) 5 cycles (b) 10 cycles (c) 15 cycles for pH 2 buffer solutions

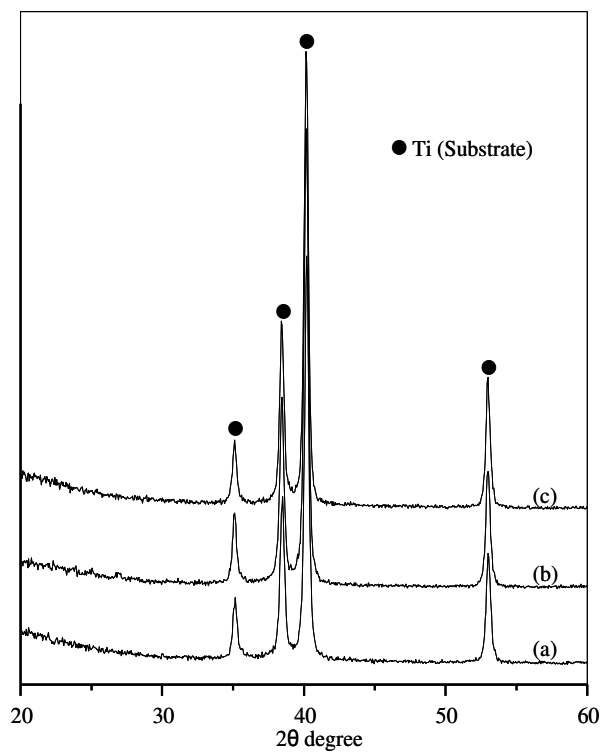


Figure 6. XRD peaks of the specimens treated electrochemically by cyclic voltametry for (a) 5 cycles (b) 10 cycles (c) 15 cycle for pH 7 buffer solutions

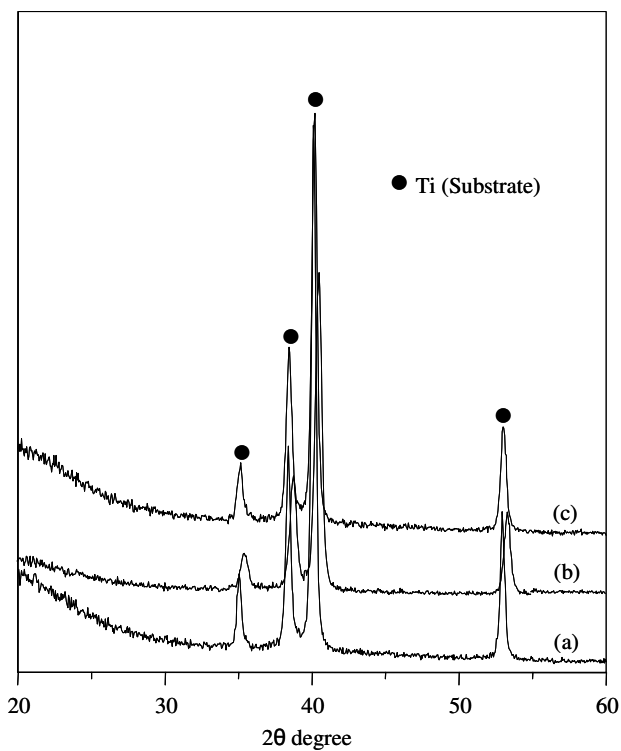


Figure 7. XRD peaks of specimens treated electrochemically by cyclic voltametry for (a) 5 cycles (b) 10 cycles (c) 15 cycle for pH 12 buffer solutions

3.3. X-ray Diffraction

The X-ray diffraction patterns were recorded for pure titanium after CV cycling between potentials of -1.0 V to +5.0 V after a different number of cycles in 0.1 M phosphate buffer solutions of pH 2, 7 and 12. Figure 5 shows intense rutile peak of TiO₂ after 5 cycles but shows only the corresponding peaks of pure titanium at pH 2 after 10 and 15 cycles. This is because at low sweep rates, the degree of order in the films increases substantially. However, at high sweep rates, the rate of dissolution of oxide film may compete with the rate of its formation. At pH 7, the XRD pattern shows only peaks for pure titanium after different repetitive cycles (Figure 6). Similarly, Figure 7 shows the XRD pattern at pH 12. Only the corresponding peaks for pure titanium were observed in all repetitive potentiodynamic cycles. This indicates that the potentiodynamic oxidation reaction after applying an electrical potential at a lower voltage could be beneficial in achieving a higher degree of TiO₂ crystallization. Among them, the TiO₂/Ti film electrode formed at 5.0 V at pH 2 for 5 cycles had the most regular crystal structure of rutile phase. Amorphous titania was formed under the other conditions.

4. CONCLUSIONS

The voltammetric experiments have shown the formation of an anodic deposit on titanium anode at three different pH in phosphate buffer solution. SEM micrograph showed that the corrosion of metal increases with increasing the number of cycles at pH 2. The corrosion was more uniform at higher number of cycles. Similarly, there were no changes in the level of corrosion at pH 7 and decreases at pH 12 as the number of potentiodynamic cycles increased. Similar trend was seen in surface roughness. The composition of oxide film consists of rutile TiO₂ after 5 potentiodynamic cycles at pH 2 but in other cases amorphous TiO₂, as shown by the XRD pattern. The results so far indicate that the corrosion of titanium and surface roughness of modified surface were dependent on electrolyte pH and number of potentiodynamic cycles.

ACKNOWLEDGEMENTS

This work was supported by a Korea Science and Engineering Foundation (KOSEF) grant funded by the Korean government (MOST) (No. R01-2007-000-20488-0).

References

1. ASM Handbook Committee, *Metals Handbook—Corrosion of Metallic implants and Prosthetic Devices*, vol. 13, ninth ed., American Society for Metals, Metals Park, 1987.
2. K. J. Bundy, *Crit. Rev. Biomed. Eng.*, 22 (3/4) (1994) 139.
3. K. Bordji, J.Y. Jozeau, D. Mainard, E. Payar, P. Nether, T. Stucky, and M. age Ali, *Biomaterials*, 17 (1996) 929.
4. Kitsugi, T. Nakayama, M. Oka, W. Q. Yan, T. Goto, T. Shibuya, T. Kokubo, and S. J. Miyaji, *Biomed. Mater. Res.*, 32 (1996)149.

5. M. Browne, J. Gregson, and R. H. Weat, *J. Mater. Sci.: Mater. Med.*, 7 (1996) 323.
6. R. M. Pilliar, *J. Biomed. Mater. Res. Appl. Biomater.*, 21 (1987)1
7. R. M. Pilliar, *Int J Powder Metal*, 34 (1998) 33.
8. C. A. Simmons, N. V. Valiquette, and R. M. Pilliar. *J Biomed Mater Res*, 47 (1999) 127.
9. Y. Z. Yang, J. M. Tian, J. T. Tian, Z. Q. Chen, X. J. Deng, and D. H. Zhang. *J. Biomed. Mater. Res.*, 52 (2000) 333.
10. L. D. Piveteau, B. Gasser, and L. Schlapbach. *Biomaterials*, 21 (2000) 2193.
11. T. Jinno, V. M. Goldberg, D. Davy, and S. Stevenson. *J. Biomed. Mater. Res.*, 42 (1998) 20.
12. D.G. Kolman, and J. R. Scully, *J. Electrochem. Soc.*, 142 (1995) 2179.
13. E. M. Patrito, R. M. Torresi, E. P. M. Leiva, and V. A. Macagno, *J. Electrochem. Soc.*, 137 (1990) 524.
14. E. Kelly, in: J. O. M. Bockris, B. E. Conway, and R. White (Eds.), *Modern Aspects of Electrochemistry*, Plenum, New York, 1982, p. 319.
15. J. Pan, D. Thierry, and C. Leygraf, *Electrochim. Acta*, 41 (1995)1143.
16. D. J. Blackwood, L. M. Peter, and D. E. Williams, *Electrochim. Acta*, 33 (1988) 1143.
17. S. Ferdjani, D. David, and G. Beranger, *J. Alloys Compd.*, 200 (1993) 191.
18. L. D. Arsov, C. Kormann, and W. Plieth, *J. Electrochem. Soc.*, 138 (1991) 2964.
19. C. P. De Pauli, M. C. Giordano, and J. O. Zerbino, *Electrochim. Acta*, 28 (1983) 1781.
20. S. H. Bonilha, and C. F. Zinolla, *Electrochim. Acta*, 43 (1998), 423.
21. D. J. Blackwood, and L. M. Peter, *Electrochim. Acta*, 34 (1989) 1505.
22. A. Müller, G. S. Popkirov, R. N. Schindler, and Ber. Bunsenges. *Phys. Chem.*, 96 (1992)1432.
23. C. P. De Pauli, M. C. Giordano, and J. O. Zerbino. *Electrochim. Acta*, 28 (1983) 1781.
24. M. A. Abdel-Rahim, *J. Appl. Electrochem*, 25 (1995) 881.
25. M. Pourbaix, *Atlas of Electrochemical Equilibria in Aqueous Solutions*, ACE; Houston, 1974.
26. F. Di Quarto, S. Piazza, and C. Sunseri, *Electrochim. Acta*, 35 (1990) 99.
27. S. R. Biaggio, N. Bocchi, R. C. Rocha-Filho, and F. E. Varela, *J. Braz. Chem. Soc.*, 8 (1997) 615.
28. S. Kudelka, A. Michaelis, and J. W. Schultze, *Electrochim. Acta*, 41 (1996) 63.
29. S. Kudelka, and J. W. Schultze, *Electrochim. Acta*, 42 (1997) 2817.
30. O. R. Camara, C. P. De Pauli, and M. C. Giordano, *Electrochim. Acta*, 29 (1984)1111.
31. M. M. Lohrengel, *Electrochim. Acta*, 39 (1994) 1265.